

Structural, electronic, and magnetic properties of Fe₁₆N₂

Hideaki Sawada,* Atsushi Nogami, and Tooru Matsumiya
*Advanced Materials & Technology Research Laboratories, Nippon Steel Corporation,
 1618 Ida, Nakahara-ku, Kawasaki 211, Japan*

Tamio Oguchi

Department of Materials Science, Hiroshima University, 1-3-1 Kagamiyama, Higashi-Hiroshima 724, Japan
 (Received 10 March 1994; revised manuscript received 25 May 1994)

The crystal structure of Fe₁₆N₂ was optimized by calculating atomic forces on the basis of an augmented-plane-wave force method. We found interesting cooperative structural relaxations of the iron atoms around the nitrogen, though the optimized structure is not far from the experimental proposal. Calculated hyperfine fields for each iron site for the optimized Fe₁₆N₂ show an interesting systematic feature when compared with experimental results.

I. INTRODUCTION

Since a large magnetization was reported for Fe₁₆N₂ by Kim and Takahashi,¹ much attention has been paid to reproduce such a magnetization experimentally.²⁻⁶ Sugita *et al.* succeeded in making a single crystal of Fe₁₆N₂ by a molecular-beam-epitaxy technique.³ The saturation flux density B_s of the sample was measured to be 3.2 T, corresponding to an average magnetic moment of $3.5\mu_B$ per iron atom at liquid helium temperature. On the other hand several band-structure calculations have also been done to elucidate the microscopic origin of the large magnetization.⁷⁻¹¹ However, the calculated average magnetic moments per iron atom are in a range 2.4-2.5 μ_B , which are considerably smaller than the experimentally estimated values. In all of these calculations the lattice constants and internal structural parameters were assumed to be the ones obtained experimentally by Jack.¹² The precise positions of iron atoms around a nitrogen atom have not been well established, because the Fe₁₆N₂ phase is not thermodynamically stable. The proposed crystal structure of the Fe₁₆N₂ phase can be regarded as that of tetragonally distorted bcc iron with ordered nitrogens at the octahedral sites. It is well known that the magnetic moment may be very sensitive to local lattice relaxations, especially in a system with interstitial impurities.^{13,14}

In this work, we optimize the internal structural parameters of iron sites in Fe₁₆N₂ and study the electronic and magnetic properties in relation to the large magnetization. The optimized structural parameters are not far from Jack's positions but important cooperative relaxations of iron atoms were found around the nitrogen. The magnetic moments within the assumed muffin-tin spheres change slightly by the structural optimization but no change occurs in the total or average magnetic moment. The difference between the calculated and the experimental hyperfine fields at the iron and nitrogen sites in Fe₁₆N₂ indicates systematics which is also consistent with pure bcc iron.

II. CALCULATIONAL METHOD

We carried out atomic force calculations using an augmented-plane-wave (APW) force method recently proposed by Soler and Williams.^{15,16} As already shown in several applications,^{17,18} the APW forces are sufficiently accurate and reliable with a moderate number of the plane waves. Since the only two internal parameters are degrees of freedom to be determined within the body-centered-tetragonal structure in the present system, we do not utilize a dynamical optimization procedure but simply calculate atomic forces for several different atomic configurations near the equilibrium and fit them to a form of

$$F_{\alpha i} = - \sum_{\beta j} \frac{\partial^2 E}{\partial R_{\alpha i} \partial R_{\beta j}} \Delta R_{\beta j} + O(\Delta R^2), \quad (1)$$

where $\Delta R_{\beta j}$ is the displacement of the atom β in the direction j from its equilibrium position. From the obtained force constants $\partial^2 E / (\partial R_{\alpha i} \partial R_{\beta j})$, the corresponding phonon modes to the displacements can be analyzed by diagonalizing the adiabatic dynamical matrix,

$$D_{\alpha i, \beta j} = (M_{\alpha} M_{\beta})^{-\frac{1}{2}} \frac{\partial^2 E}{\partial R_{\alpha i} \partial R_{\beta j}}, \quad (2)$$

In this calculation, 12 \mathbf{k} points in the irreducible Brillouin zone and a Gaussian broadening scheme with a width of 5 mRy were used to sum up the occupied states. For the exchange-correlation part of the local spin density approximation the approach of Hedin and Lundquist is employed.¹⁹ In the Soler-Williams representation for the Kohn-Sham wave function, the plane waves are allowed to penetrate into the muffin-tin spheres. Due to this virtue, the angular momentum in the spherical-wave expansion can be truncated at $l_{\max} = 2$ in the present system. The energy cutoff of 15 Ry, corresponding to about 680 plane waves, was used for the wave function.

TABLE I. The positions of iron and nitrogen sites of Fe_{16}N_2 .

Site	Positions
Fe[4(e)]	$(0, 0, z)(\frac{1}{2}, \frac{1}{2}, \frac{1}{2} + z)(0, 0, -z)(\frac{1}{2}, \frac{1}{2}, \frac{1}{2} - z)$
Fe[8(h)]	$(x, x, 0)(\frac{1}{2} + x, \frac{1}{2} + x, \frac{1}{2})(x, -x, 0)(\frac{1}{2} + x, \frac{1}{2} - x, \frac{1}{2})$
Fe[4(d)]	$(0, \frac{1}{2}, \frac{1}{4})(\frac{1}{2}, 0, \frac{3}{4})(\frac{1}{2}, 0, \frac{1}{4})(0, \frac{1}{2}, \frac{3}{4})$
N[2(a)]	$(0, 0, 0)(\frac{1}{2}, \frac{1}{2}, \frac{1}{2})$

The numerical parameters are sufficient to obtain convergence of the magnetic moment and geometry within a few percent error from the previous calculation.¹⁸ The muffin-tin sphere radii of iron and nitrogen are chosen to be 1.0 and 0.8 Å, respectively. The magnetic moment and lattice constant of bcc iron are in good agreement with the experimental results.

III. RESULTS AND DISCUSSION

A. Structural optimization

Fe_{16}N_2 has a body-centered-tetragonal structure with three types of iron sites [4(e), 8(h), 4(d)] as drawn in Fig. 1.¹² The atomic positions of the iron and nitrogen atoms proposed by Jack¹² are listed in Table I. The observed x-ray reflection intensities are well fitted to those calculated with values of $z=0.3125$ and $x=0.25$ (called Jack-1). But he pointed out that no worse agreement between the observed and calculated intensities was obtained by taking $x=0.222$ and $z=0.306$ (Jack-2). Therefore the structural parameters x and z are not determined precisely only by experimental techniques. In this study

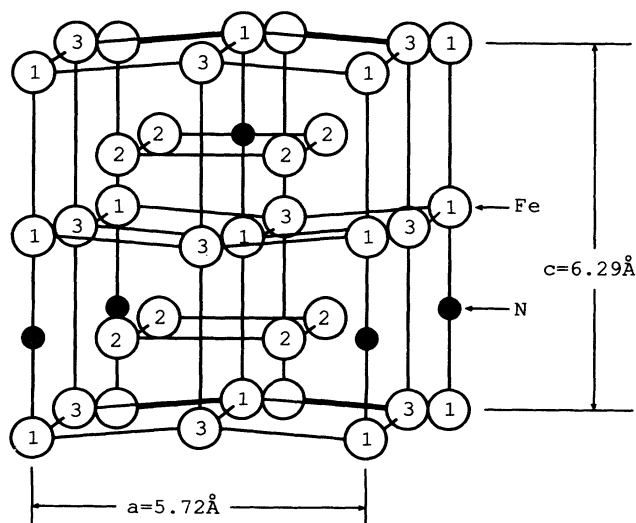


FIG. 1. Crystal structure of Fe_{16}N_2 . Fe-1, Fe-2, and Fe-3 correspond to Fe[4(e)], Fe[8(h)], and Fe[4(d)], respectively.

TABLE II. The structural parameters x and z of Fe_{16}N_2 .

	Jack-1	Jack-2	Optimized
x	0.25	0.222	0.243
z	0.3125	0.306	0.293

the parameters x and z are optimized so that the atomic forces acting on Fe[4(e)] and Fe[8(h)] vanish. The optimized x and z values, and the distance of atomic pairs are listed in Tables II and III, respectively. There are two kinds of the nearest Fe[4(e)]-Fe[8(h)] distance, 2.820 and 2.341 Å for Jack-1. The shorter one, 2.341 Å, is extremely shorter than the nearest iron-iron distance of bcc iron, 2.477 Å. Therefore the crystal structure of Jack-1 is not expected to be stable due to a large elastic energy. After the optimization, the Fe[4(e)]-Fe[8(h)] distance becomes closer to the iron-iron distance in bcc iron. Since the Fe[4(e)]-Fe[4(e)] distance of Jack-1 is also shorter than the iron-iron distance in bcc iron, it may be elongated more or less. As for the distances between iron and nitrogen, the distance of Fe[4(e)]-N[2(a)] becomes shorter by the optimization. The optimized Fe[4(e)]-N[2(a)] distance is remarkably close to the nearest iron-nitrogen distance of Fe_4N , 1.898 Å.

This sequence of the relaxations of the Fe[8(h)] and Fe[4(e)] atoms can be understood as a cooperative relaxation mechanism starting the ideal bct structure with nitrogens at the octahedral interstitial sites, as illustrated schematically in Fig. 2. At the ideal positions of the bct structure, $z=0.25$ and $x=0.25$, neighboring Fe[4(e)] and nitrogen atoms are too close to each other. The Fe[4(e)] atoms move first farther from the nitrogen. Due to this movement, the nearest two Fe[4(e)] atoms get closer and squeeze the nearest Fe[8(h)] atoms toward a nitrogen at the opposite side. As a result, the Fe[8(h)]-N[2(a)] distance becomes shorter than the ideal one.

The optimized structure is more stable than Jack-1 by 62.4 mRy per Fe_{16}N_2 . It is known experimentally that Fe_{16}N_2 decomposes to ferrite iron and Fe_4N . We also calculated the total energies of bcc iron and Fe_4N . It is consistent with the experimental results that the optimized Fe_{16}N_2 is slightly less stable than bcc iron and Fe_4N by 0.8 mRy per Fe_{16}N_2 .

Fe_{16}N_2 has $3 \times 9 - 3 = 24$ optical modes represented by

$$2A_{1g} + A_{2g} + 3A_{2u} + B_{1g} + 2B_{2g} + B_{2u} + 3E_g + 4E_u, \quad (3)$$

TABLE III. Distance of atomic pairs. Units of Å are used.

	Jack-1	Jack-2	Optimized
Fe[4(e)]-Fe[8(h)]	2.820	2.632	2.695
	2.341	2.559	2.453
Fe[8(h)]-Fe[4(d)]	2.562	2.572	2.562
Fe[4(e)]-Fe[4(e)]	2.359	2.441	2.604
Fe[8(h)]-Fe[8(h)]	2.86	2.540	2.780
	2.86	3.180	2.940
Fe[4(e)]-N[2(a)]	1.966	1.925	1.843
Fe[8(h)]-N[2(a)]	2.022	1.796	1.966

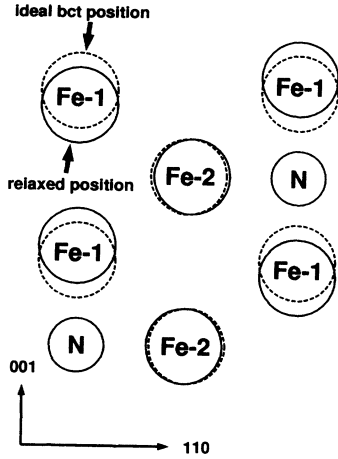


FIG. 2. Schematic view of the cooperative relaxation.

and there are two A_{1g} phonon modes related to the two structural parameters z and x . The A_{1g} phonon modes were obtained from the force constants via Eqs. (1) and (2). One of the two A_{1g} phonon modes is that Fe[4(*e*)] and Fe[8(*h*)] atoms breathe around the nitrogen simultaneously with a frequency of 11.19 THz. The other mode is that the Fe[4(*e*)] and Fe[8(*h*)] atoms move in antiphase with a frequency of 6.95 THz. Since there is no experiment to our knowledge for phonon in Fe_{16}N_2 , we cannot compare the calculated results with experiment. From the fact that the calculated phonon frequencies for iron are in very good agreement with the experiments,¹⁸ the calculated phonon modes can be good expectations.

B. Magnetic properties

The magnetic moments at iron and nitrogen sites of the structure Jack-1 and the optimized structure are summarized in Table IV with the muffin-tin radii of iron and

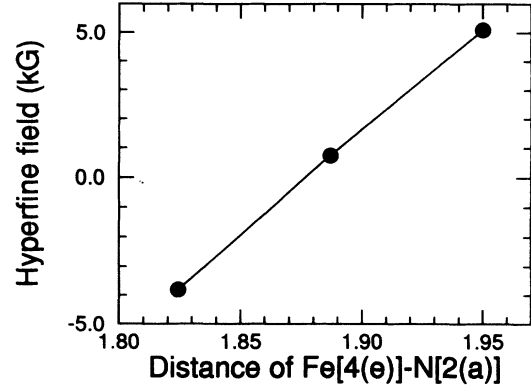


FIG. 3. Calculated hyperfine field for nitrogen as a function of distance of Fe[4(*e*)]-N[2(*a*)]. The Fe[8(*h*)]-N[2(*a*)] distance is fixed to be 2.022 Å.

nitrogen atoms. It can be seen that the structural optimization introduces a certain effect on the local magnetic moments, but nothing on the total moment. The average magnetic moment per iron is in good agreement with the previous result by a full-potential linearized augmented-plane-wave¹¹ (FLAPW) calculation, although the local magnetic moments in the present work are slightly different from those of the FLAPW calculation, because of different muffin-tin radii used. The difference in the local magnetic moments between the present and FLAPW calculations increases in the order of Fe[4(*e*)], Fe[8(*h*)], and Fe[4(*d*)]. It seems that a spatial extent of the *d* electrons increases in the order of Fe[4(*e*)], Fe[8(*h*)], and Fe[4(*d*)], that is to say, site projected density of states width is wider in the same order. In fact the tendency of the site projected density of states width was studied to be actually like that by linear-muffin-tin-orbital (LMTO) calculation.²⁰

The calculated local magnetic moments have the same tendency as the experimental values a Mössbauer measurement,⁴ although there are discrepancies between the experimental and calculated values. In this experiment the local magnetic moments were estimated by us-

TABLE IV. The muffin-tin radii (Å) and magnetic moments (μ_B) for iron and nitrogen sites of Fe_{16}N_2 .

	Expt. (Ref. 4)	Expt. (Ref. 3)	Present work		LMTO (Ref. 23)	FLAPW (Ref. 11)
			Jack-1	Optimized		
R_{Fe}				1.0	1.43	1.16
R_{N}				0.8	1.10	0.74
Fe[4(<i>e</i>)]	1.3		2.043	2.002	2.011	2.04
Fe[8(<i>h</i>)]	2.5		2.295	2.295	2.445	2.33
Fe[4(<i>d</i>)]	3.8		2.759	2.757	2.985	2.82
N[2(<i>a</i>)]			-0.058	-0.043	-0.005	-0.03
Interstitial			0.500	0.572		-0.006
Average/atom	2.5	3.5	2.403	2.403	2.471	2.37

TABLE V. The hyperfine field for iron and nitrogen sites of Fe_{16}N_2 . Units of kG are used.

	Expt.	Expt.	Present work		FLAPW
	(Ref. 4)	(Ref. 24)	Jack-1	Optimized	(Ref. 11)
Fe[4(e)]	-296		-246.4	-245.6	-243
Fe[8(h)]	-316		-245.3	-254.2	-241
Fe[4(d)]	-399		-345.7	-331.9	-334
N[2(a)]		-9.32	5.10	-7.58	

ing an assumption that the Mössbauer spectrum is determined predominantly by the local magnetic moment independent to its environment. Therefore the experimental local magnetic moment may contain ambiguity, and it is hard to compare the experimental and calculated local magnetic moments so seriously. However, the average magnetic moment has certain physical meanings, independent of the choice of muffin-tin spheres, since it can be obtained directly from the saturation magnetization. The calculated average magnetic moment turns out to be in good agreement with the experimental value in Ref. 4, while the average magnetic moment, obtained by Sugita *et al.*,³ is more than $1.0\mu_B$ larger than the calculated value. We do not know the reason for the difference of these experiments, the discrepancy between the Sugita's and the calculated values is considerably larger than that for many other compounds by Dederichs' calculation.²¹ Dederichs *et al.* calculated the magnetic properties of ferromagnetic transition metal alloys by the Korringa-Kohn-Rostoker coherent-potential-approximation (KKR-CPA) method and reproduce the Slater-Pauling curve precisely. Therefore the experimental magnetic moment³ cannot be explained within the local density approximation, if there were not problems in the experiments.

The calculated Fermi contact terms in the hyperfine fields are shown in Table V. The Fermi contact term turns out to be more sensitive to the structural change than the local magnetic moments. Especially, the value at the nitrogen site changes from positive to negative by the structural optimization. The Fermi contact term of a nitrogen interstitial impurity in ferromagnetic iron calculated by Akai *et al.*¹⁴ is -70 kG. We can expect that the strong dependence of the Fermi contact term at the nitrogen atom on the structural relaxation may yield the difference between these calculations, since Akai *et al.* did not take account of the structural relaxation. The Fermi contact term of nitrogen becomes in fact more negative with decrease of the iron-nitrogen distance as shown in Fig. 3.

The Fermi contact term of Fe[4(e)] is almost the same as that of Fe[8(h)] in the present and FLAPW calculation, in which the same structural parameters proposed by Jack¹² were used. On the other hand, the Fermi contact term of Fe[8(h)] is more negative than that of Fe[4(e)] by 8.6 kG for the optimized structure. This feature is consistent with the experimental result. Therefore, the crystal structure of the sample used for the Mössbauer spectroscopy measurement might be expected to be closer to the optimized crystal structure than Jack-1. This argument is based on the fact that the local spin density approximation can explain the major trends of the hyperfine field.²² In our calculations the calculated Fermi contact terms underestimate the experimental values by 50–67 kG in a systematic way as shown in Fig. 4. Therefore, the site dependence of the calculated hyperfine fields are consistent with that of the experimental values.

IV. SUMMARY

The positions of iron of Fe_{16}N_2 were optimized by using the APW force calculation and the electronic and magnetic properties were studied. The optimized structure is not far from Jack's proposal. The iron atoms are found to be relaxed cooperatively around the nitrogen atom. The crystal structure of the sample used for the electron Mössbauer spectroscopy measurement is expected to be closer to the optimized structure than the proposed structure by Jack, from the comparison of the calculated hyperfine fields for the optimized structure and Jack's structure.

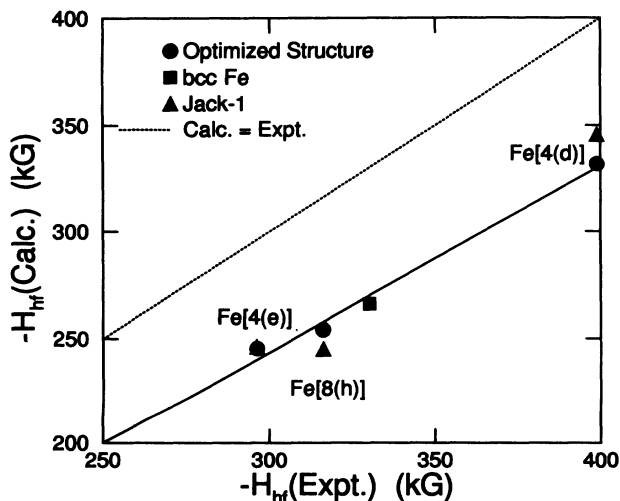


FIG. 4. Comparison of the calculated Fermi contact terms in the hyperfine field with the experimental hyperfine fields. Solid line denotes 80% of the experimental values.

- * Present address: Joint Research Center for Atom Technology, c/o NAIR 1-1-4 Higashi, Tsukuba, Ibaraki 305, Japan.
- ¹ T. K. Kim and M. Takahashi, *Appl. Phys. Lett.* **20**, 492 (1972).
- ² Y. Sugita, K. Mitsuoka, N. Komuro, H. Hoshiya, Y. Kozono, and M. Hanazono, *J. Magn. Soc. Jpn.* **15**, 667 (1991).
- ³ Y. Sugita, K. Mitsuoka, N. Komuro, H. Hoshiya, Y. Kozono, and M. Hanazono, *J. Appl. Phys.* **70**, 5977 (1991).
- ⁴ K. Nakajima, T. Yamashita, M. Takata, and S. Okamoto, *J. Appl. Phys.* **70**, 6033 (1991).
- ⁵ K. Nakajima and S. Okamoto, *J. Appl. Phys.* **65**, 4357 (1989).
- ⁶ M. Takahashi, H. Shoji, H. Takahashi, and T. Wakiyama, M. Kinoshita, and W. Ohta, *IEEE Trans. Magn.* **29**, 3040 (1993).
- ⁷ A. Sakuma, *J. Magn. Magn. Mater.* **102**, 127 (1991).
- ⁸ S. Mater, *Z. Phys. B* **87**, 91 (1992).
- ⁹ B. I. Min, *Phys. Rev. B* **46**, 8232 (1992).
- ¹⁰ S. Ishida, K. Kitawase, S. Fujii, and S. Asano, *J. Phys.: Condens. Matter* **4**, 765 (1992).
- ¹¹ R. Coehoorn, G. H. O. Daalderop, and H. J. F. Jansen, *Phys. Rev. B* **48**, 3830 (1993).
- ¹² K. H. Jack, *Proc. R. Soc. London, Sec. A* **208**, 216 (1951).
- ¹³ M. Akai, H. Akai, and J. Kanamori, *J. Magn. Magn. Mater.* **31-34**, 551 (1983).
- ¹⁴ M. Akai, H. Akai, and J. Kanamori, *J. Phys. Soc. Jpn.* **56**, 1064 (1987).
- ¹⁵ J. M. Soler and A. R. Williams, *Phys. Rev. B* **40**, 1560 (1989).
- ¹⁶ J. M. Soler and A. R. Williams, *Phys. Rev. B* **42**, 9728 (1990).
- ¹⁷ T. Oguchi and T. Sasaki, in *Computer Aided Innovation of New Materials II*, edited by M. Doyama, J. Kihara, M. Tanaka, and R. Yamamoto (North-Holland, Amsterdam, 1993), p. 107.
- ¹⁸ T. Oguchi, in *Interatomic Potential and Structural Stability*, edited by K. Terakura and H. Akai (Springer-Verlag, Berlin, 1993), p. 33.
- ¹⁹ L. Hedin and S. Lundqvist, *J. Phys. C* **4**, 2064 (1971).
- ²⁰ H. Sawada, A. Nogami, and T. Matsumiya, *J. Comput. Aid. Mater. Design* **1**, 75 (1993).
- ²¹ P. H. Dederichs, R. Zeller, H. Akai, and H. Ebert, *J. Magn. Magn. Mater.* **100**, 241 (1991).
- ²² H. Akai, M. Akai, S. Blügel, B. Drittler, H. Ebert, K. Terakura, R. Zeller, and P. H. Dederichs, *Prog. Theor. Phys. Suppl.* **101**, 11 (1990).
- ²³ H. Sawada, A. Nogami, and T. Matsumiya, in *Computer Aided Innovation of New Materials II*, edited by M. Doyama, J. Kihara, M. Tanaka, and R. Yamamoto (North-Holland, Amsterdam, 1993), p. 213.
- ²⁴ T. Minamisono, Y. Nojiri, K. Matsuta, T. Iwayama, and M. Fujinaga, *Hyperfine Interact.* **34**, 299 (1987).